Sample Ripening through Nanophase Separation Influences the Performance of Dynamic Nuclear Polarization

Emmanuelle M. M. Weber, Giuseppe Sicoli, Hervé Vezin, Ghislaine Frebourg, Daniel Abergel, Geoffrey Bodenhausen, Dennis Kurzbach

Sample Ripening through Nanophase Separation Impacts the Performance of Dynamic Nuclear Polarization

Emmanuelle M. M. Weber,[a] Giuseppe Sicoli,[b] Hervé Vezin,[b] Ghislaine Frébourg,[c] Daniel Abergel,[a] Geoffrey Bodenhausen,[a] Dennis Kurzbach[a,]*

Abstract: Mixtures of water and glycerol provide popular matrices for low-temperature spectroscopy of vitrified samples. However, they involve counterintuitive physicochemical properties, such as spontaneous nanoscopic phase separations (NPS) in solutions that appear macroscopically homogeneous. We demonstrate that such phenomena can substantially impact the efficiency of dynamic nuclear polarization (DNP) by factors up to 20% by causing fluctuations in local concentrations of polarization agents (radicals). Thus, a spontaneous NPS of water/glycerol mixtures that takes place on time scales on the order of 30-60 min results in a confinement of polarization agents in nanoscopic water-rich vesicles, which in return affects the DNP. Such effects were found for three common polarization agents, TEMPOL, AMUPol and Trityl.

Mixtures of water and organic solvents may feature unusual physicochemical events like spontaneous nanophase separations (NPS)[1] that occur in solutions despite their homogenous appearance on a macroscopic scale.[2] Such NPS describe rather counterintuitive phenomena, where the two components of a binary solvent mixture spontaneously form co-existing metastable transient nanophases. The intriguing nature of NPS recently fostered much academic interest.[3] In this work, we show how such phenomena can impact the performance of dynamic nuclear polarization (DNP), a method to enhance the sensitivity of nuclear magnetic resonance (NMR) by boosting the nuclear spin polarization *P*, i.e., the relative difference between the populations of the excited and ground spin states. DNP has recently witnessed significant developments, allowing one to achieve ever-higher levels of polarization due to (1) instrumental developments and (2) novel polarization agents (PAs) such as bi-nitroxides or tri-aryl-methyl radicals, also known as "Trityls". These developments provide access to systems that could not be studied before by NMR due to poor sensitivity.

[a] Ms. EMM Weber, Dr D Abergel, Prof. G Bodenhausen, Dr D. Kurzbach
Laboratoire des biomolécules, LBM, Département de chimie, École normale supérieure, PSL University, Sorbonne Université, CNRS, 75005 Paris, France
E-mail: Kurzbach@ens.fr
[b] *Dr Giuseppe Sicoli, Dr Hervé Vezin*
Université Lille, UMR CNRS 8516 - LASIR, Laboratoire de Spectrochimie Infrarouge et Raman, F-59000 Lille, France.
[c] Mrs. G Frébourg
Institut de Biologie Paris-Seine, Sorbonne Université / CNRS
Campus Pierre et Marie Curie, 7-9 quai St Bernard
75252 PARIS, France

Supporting information for this article can be obtained via a link at the end of the document.

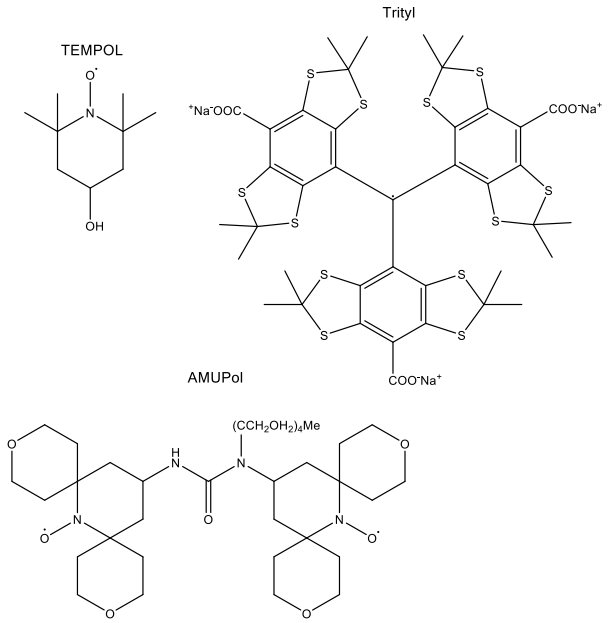

Figure 1. Three polarization agents that are commonly used for DNP.

Water/glycerol mixtures that contain concentrations of PAs[4] of 10 – 80 mM are frequently used as low-temperature DNP matrices. We here show that such sample preparations can feature distributions of radicals that are heterogeneous on nanometric length scales as a consequence of "ripening" effects that lead to the emergence of two co-existing phases that may have different local PA concentrations. We find that water/glycerol mixtures can indeed lead to the formation of nanoscopic water vesicles dispersed in a glycerol-rich matrix, which can be trapped during the vitrification step that precedes low-temperature DNP. As a result, the local PA concentration in water- and proton-rich phases varies, which impacts DNP performances. Such behavior can be of importance in many fields of research, such as dissolution DNP of biomolecules,[5] drug screening,[5b, 6] *in-vivo* imaging[7] and cancer monitoring,[8] since many of these studies employ water-glycerol mixtures.[9]

The transient accumulation of various molecular agents in an environment that is confined on a nanometric scale may not only improve DNP, but may also serve other technologies such as transiently formed nanostructures,[10] shelters[11] or reactors[12] by increasing the selectivity and specificity of chemical reactions under investigation.

The here studied DNP samples consisted of a mixture of 50% v/v glycerol-d_8 and 50% v/v of a solution of one of the following PAs in 80% D_2O and 20% H_2O: **I**) 100 mM TEMPOL (4-hydroxy-2,2,6,6-tetramethylpiperidin-1-oxyl), **II**) 40 mM AMUPol (15-{[(7-oxyl-3,11-dioxa-7-azadispiro[5.1.5.3]hexadec-15-yl)carbamoyl][2-(2,5,8,11-tetraoxatridecan-13-ylamino)}-[3,11-dioxa-7-azadispiro[5.1.5.3]hexadec-7-yl])oxidanyl) and **III**) 30 mM Trityl (OX063) (see Fig. 1). The solutions were stirred during ca. 60 s at 22.5 ˚C until they appeared macroscopically homogeneous. To study the influence of ripening on the preparations, the samples were allowed to rest at 22.5 ˚C for a

suitable "ripening interval" T_{ripe}, which can be on the order of minutes to hours. Subsequently, they were "flash vitrified" in liquid helium at 4.2 K for DNP.

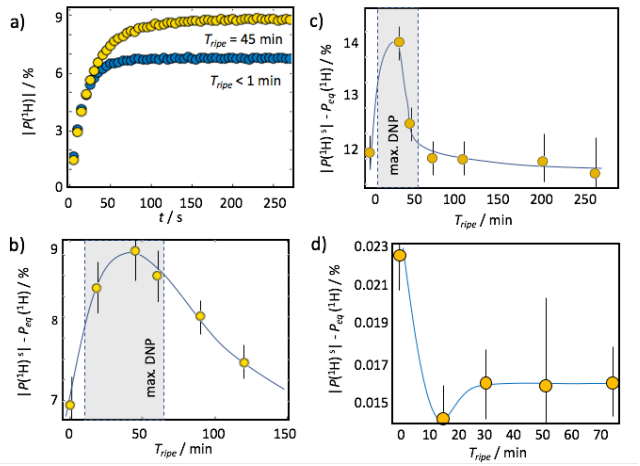

Figure 2. a) Build-up curves of the proton polarization $|P(^1H)^s|$ induced by microwave saturation (187.9 GHz with a 2 kHz frequency modulation over a bandwidth of 100 MHz) of the EPR transitions of 50 mM TEMPOL at 4.2 K and 6.7 T. Blue: Sample vitrified immediately after preparation (T_{ripe} < 1 min). Yellow: Sample vitrified after a ripening interval T_{ripe} = 45 min following sample preparation. b) Difference $|P(^1H)^s|$ - $P_{eq}(^1H)$ between absolute steady-state proton polarization $|P(^1H)^s|$ and thermal equilibrium polarization P_{eq} at 4.2 K as a function of the interval T_{ripe} between preparation and vitrification of the water glycerol/mixtures. The solid line serves to guide the eye. Similar results have been reproduced in three independent experiments (see the Supporting Information). c) Difference $|P(^1H)^s|$ - $P_{eq}(^1H)$ versus T_{ripe} for 20 mM AMUPol at 4.2 K. d) Difference $|P(^1H)^s|$ - $P_{eq}(^1H)$ versus T_{ripe} for 15 mM trityl at 4.2 K. In this case, one observes a drop of ca. 43% for T_{ripe} = 15 min.

The duration of the "ripening interval" T_{ripe} has important effects on the proton polarization level in DNP experiments as shown in Fig. 2a for sample **I**, containing 50 mM TEMPOL, where we find more efficient DNP for T_{ripe} = 45 min in comparison to T_{ripe} < 1 min. Fig. 2b displays the dependence of the proton polarization $|P(^1H)^s|$ on the ripening interval. The highest polarization is achieved for 40 min < T_{ripe} < 60 min. In comparison to polarization levels obtained for T_{ripe} < 1 min or for T_{ripe} > 4 h, gains in $|P(^1H)^s|$ from 7 to 9% at 4.2 K and 6.7 T translate into a gain of more than 20% in the NMR signal enhancement factor ε.[13]

Fig. 2c displays a similar profile for sample **II** containing 20 mM AMUPol. Here, we observe a maximum DNP performance after a ripening interval 30 < T_{ripe} < 50 min. The enhancement factor ε is improved by ca. 17% when $|P(^1H)^s|$ increases from 12% to 14%. In stark contrast, for sample **III** (Fig. 2d) containing 15 mM Trityl, we observed a 40% *decrease* of $|P(^1H)^s|$ for T_{ripe} = 15 min. Unlike for TEMPOL and AMUPol, the EPR line of Trityl is narrower than the proton Larmor frequency. Hence, the solid effect (SE) is dominant for Trityl, while thermal mixing (TM) dominates for the nitroxides under our experimental conditions. This has two consequences: 1. the SE is less effective than TM because the build-up rate of $|P(^1H)^s|$ is on the same order as the proton relaxation rates $R_1(^1H)$ and 2. the dependence of the DNP efficiency on the local PA concentration is not the same for SE and TM mechanisms. Indeed, contrary to samples **I** and **II** the difference $|P(^1H)^s|$ - $P_{eq}(^1H)$ drops from only 0.023% at T_{ripe} = 0 to 0.013% at T_{ripe} = 15 min before stabilizing around 0.016% after T_{ripe} = 30 min. Despite the obvious differences between Trityl and the two nitroxides under investigation, we again observe a ripening process on a time scale of 30 - 60 min. (Note that we observed ripening also at lower global radical concentrations; see the Supporting Information). This fact should henceforth be considered in DNP optimization studies.

To cast light on the processes underlying our observations, we studied the time evolution of the nanoscopic morphology of the DNP samples by cryo-transmission electron microscopy (TEM). We prepared similar samples and vitrified them at 90 K in liquid ethane after different intervals T_{ripe}. For T_{ripe} = 0 or 240 min (Fig. 3a and b) we observed a homogeneous morphology of the water/glycerol mixture by cryo-TEM. However, the DNP samples undergo morphological transitions during ripening leading to the spontaneous formation of spherical water vesicles of ca. 10-50 nm diameter (Fig. 3c). A similar phenomenon of demixing and subsequent remixing, was reported by Murata and Tanaka.[2] For 20 < T_{ripe} < 45 min, we clearly observed the nanoscopic separation

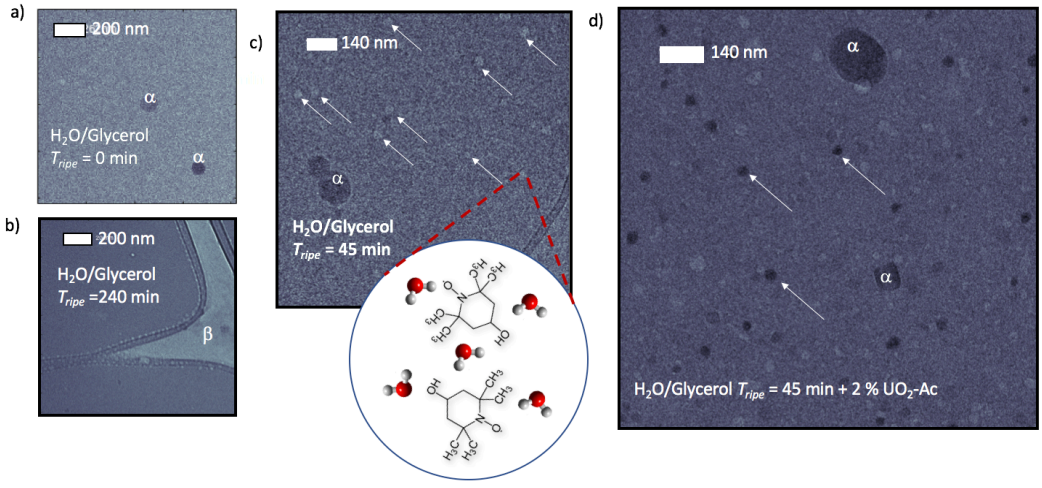

Figure 3. Cryo-TEM pictures of morphological changes due to nanophase separation (NPS) resulting from ripening during an interval T_{ripe} between mixing at room temperature and rapid vitrification by plunging the samples into liquid ethane at 90 K. For T_{ripe} = 0 min (a) or 240 min (b), no NPS could be observed. The letter α on the figure indicates ethane droplets on the vitrified film. The letter β indicates the carbon support grid. c) Water-rich phases (in which the TEMPOL radicals are confined) appear as light vesicles at T_{ripe} = 45 min, indicated by white arrows. d) Addition of 2% uranyl acetate stains the water-rich vesicles by a dark contrast as indicated by the white arrows.

of a water-rich phase (vesicles) and a glycerol-rich phase (matrix, Fig 3c).

We only observed such a formation of vesicles for glycerol contents of 40-50% v/v, since cryo-TEM is not possible at 60% v/v as the glass transition temperatures becomes too low.

To confirm the formation of water-rich phases, we employed negative staining techniques using the hydrophilic uranyl ion (UO_2^{2+}), which preferentially accumulates in water-rich environments. In Fig. 3d, the water vesicles are stained in a darker shade due to the presence of the heavy ions, thereby corroborating the observation of NPS in the DNP samples.

Note that the hyperpolarization build-up time in Fig. 1a appears longer for T_{ripe} = 45 min than for T_{ripe} = 0. This is likely a consequence of NPS, as shown by Ji et al.[14] for heterogeneous samples, where PA-depleted phases feature slow build-up processes when they are spatially separated from PA-rich phases featuring faster build-up processes.

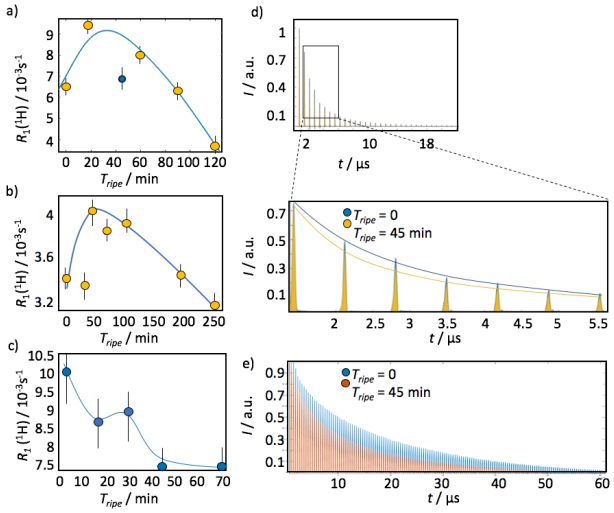

Figure 4. Local PA distribution. a) $R_1(^1H)$ as a function of the ripening interval for sample **I**. Between T_{ripe} = 20 min and 60 min, increased relaxation rates for protons can be observed, confirming that the local PA concentration is increased due to NPS. At T_{ripe} = 45 min the decay showed a bi-exponential behavior (blue point indicates the fast component; the slow component was $8.4 \cdot 10^{-4}$ s^{-1}; not shown for the sake of visibility; see Supporting Information). The blue line serves to guide the eye. b) The longitudinal relaxation rate $R_1(^1H)$ as a function of the ripening interval for sample **II**. An increase can be observed for 30 min < T_{ripe} < 100 min. The blue line guides the eye. c) $R_1(^1H)$ as a function of the ripening interval for sample **III**. The blue line is again to guide the eye. d) Transverse electron spin relaxation rates $R_{2e} = 1/T_{2e}$ of 10 mM TEMPOL measured at 77 K using a CPMG pulse sequence after T_{ripe} = 0 (blue dots) and T_{ripe} = 45 min (yellow dots). The black box indicates the enlarged region shown below. The solid blue and yellow lines indicate the signal envelopes to which R_{2e} was fitted. R_{2e} raises for T_{ripe} = 45 min, indicating increased local radical concentrations. e) Same as in d), but for sample **III**. Again, ripening effects are clearly observed and relaxation is faster for T_{ripe} = 45 min.

Fig. 4a and b show that the longitudinal proton relaxation rate $R_1(^1H)$ at 4 K and 6.7 T increases due to NPS for samples **I** and **II** containing TEMPOL and AMUPol. This occurs between T_{ripe} = 20 and T_{ripe} = 60 min for sample **I** and between T_{ripe} = 40 and T_{ripe} = 100 min for sample **II**. This finding indicates a local increase in PA concentration (depending on the ripening interval) in proton-rich environment, i.e., in the water vesicles, based on the fact that for the mono radical TEMPOL, the proton relaxation rate at 4.2 K is predominantly determined by electron-proton flip-flop transitions.[9] Therefore, since the relaxation rates increase by ca. 20% due to ripening of sample **I**, the PA concentration must increase in the water vesicles during NPS, since all other parameters (temperature, overall concentrations, etc.) remain unchanged. For sample **II**, the presence of two coupled radicals in the PA complicates the relaxation behavior as three-spin processes are fostered, yet a qualitatively similar concentration dependence can be expected. In contrast, for sample **III** (Trityl, Fig. 4c) we find a *decrease* of $R_1(^1H)$ from 10 to ca. $7.5 \cdot 10^{-3}$ s^{-1} between T_{ripe} = 0 and T_{ripe} = 40 min. As the DNP performance also decreases for Trityl (Fig. 1) between T_{ripe} = 0 and T_{ripe} = 30 min, in contrast to samples **I** and **II**, it is likely that the Trityl radicals are accumulated in the glycerol-rich phase and, hence, separated from the protons in the water-rich phase that we observe by NMR, so that proton relaxation decelerates upon NPS.

Note that, also from the viewpoint of relaxation, all three samples again show ripening in water/glycerol mixtures with distinct features for 15 < T_{ripe} < 60 min. Interestingly, we find bi-exponential relaxation behavior for sample **I** when $|P(^1H)^s|$ reaches a maximum at T_{ripe} = 45 (see blue data point in Fig. 4a and Supporting Information) indicating that spin diffusion cannot cover the entire sample due NPS.

Assuming a perfect phase separation and an even distribution of all labile protons and deuterons in the sample - which might be an oversimplification, since the water-glycerol proton/deuterium exchange (H/D exchange) might proceed on a similar or longer timescale as the NPS reported here - the proton concentration in the water-rich phase would be 5 times higher than in the glycerol-rich phase. Slow H/D exchange would further boost the local ^1H concentration, since all samples were prepared with fully deuterated glycerol and partly deuterated water so that slow exchange would further increase the local ^1H concentration in the water vesicles. Hence, not only PAs but also protons become enriched in the water-rich phases due to NPS.

In a next step, we measured the transverse electronic relaxation rates $R_{2,e}$ of the PAs as a function of T_{ripe} by means of pulsed electron paramagnetic resonance (EPR) experiments, for which the samples were prepared with the same protocol as for DNP, but vitrified in liquid nitrogen. Fig. 4d shows that $R_{2,e}$ increases for sample **I** from $4.9 \cdot 10^5$ to $5.8 \cdot 10^5$ s^{-1} when going from T_{ripe} = 0 to 45 min. Thus, in comparison to samples with T_{ripe} < 1 min, the transverse electronic relaxation rates $R_{2,e}$ of the radicals becomes faster. As the rates $R_{2,e}$ primarily depend on the local radical concentration and their mutual dipolar couplings (*ceteris paribus*), increased $R_{2,e}$ rates indicate stronger couplings corresponding to locally increased concentrations of TEMPOL in the aqueous phase. For sample **II** we determined that the relaxation rates are independent of T_{ripe} as the electronic relaxation is likely to be dominated by concentration-independent intramolecular dipolar couplings. For 5 mM AMUPol $R_{2,e}$ barely varied, from $2.6 \cdot 10^5$ s^{-1} to $2.5 \cdot 10^5$ s^{-1} between T_{ripe} < 1 min and 45 min, respectively. For the Trityl, sample **III,** we again observed ripening via electronic relaxation as displayed in Fig. 4e. For 5 mM Trityl the $R_{2,e}$ rate increased from $8.3 \cdot 10^4$ s^{-1}

to $1.3 \cdot 10^5$ s^{-1} between T_{ripe} = 0 and 45 min. Hence, sample ripening influences the electronic relaxation rates of both mono-radicals indicating clustering and increased local PA concentrations due to NPS.

To corroborate these findings, we systematically varied the water-glycerol ratio. The effect on continuous-wave EPR spectra recorded at 120 K after T_{ripe} = 45 min confirm a preferential accumulation of TEMPOL and AMUPol in the water-rich phase, while Trityl accumulates in the water-depleted phase (see Supporting Information.)

Finally, we ran preliminary studies on sample **I** based on double electron-electron resonance (DEER) (see *Supporting Information*)[15] which allows one to measure distance-dependent dipolar couplings between electrons. After sample ripening, a non-homogeneous distribution of short distances was observed for TEMPOL, while for T_{ripe} < 1 min the distribution was found to be more homogeneous, again highlighting the local accumulation of PAs during the NPS.

Acknowledgements

The authors thank Prof. Jacques Dubochet (Université de Lausanne) for his advice on cryo-EM data. We thank Dr. Yves-Michel Frapart (Université Paris-Descartes) for providing Trityl radicals. This work was supported by the CNRS research infrastructure RENARD (FR 3443) for EPR facilities and financed by the French CNRS and the European Research Council (ERC contract “Dilute Para-Water”). We thank Bruker BioSpin for providing the DNP equipment and the EM Service of the IBPS (CNRS FR 3631) at UPMC.

Keywords: Phase Separation • Dynamic Nuclear Polarization • DNP Juice • Nanophases • Nuclear Magnetic Resonance

[1] a) D. A. Jahn, J. Wong, J. Bachler, T. Loerting, N. Giovambattista, *Phys Chem Chem Phys* **2016**, *18*, 11042-11057; b) J. Bachler, V. Fuentes-Landete, D. A. Jahn, J. Wong, N. Giovambattista, T. Loerting, *Phys Chem Chem Phys* **2016**, *18*, 11058-11068; c) K. Murata, H. Tanaka, *Nat Mater* **2012**, *11*, 436-443.

[2] K. Murata, H. Tanaka, *Nat Commun* **2013**, *4*, 2844 1-8.

[3]a) N. Severin, J. Gienger, V. Scenev, P. Lange, I. M. Sokolov, J. P. Rabe, *Nano Lett* **2015**, *15*, 1171-1176; b) Z. Zhao, C. A. Angell, *Angew Chem Int Ed Engl* **2016**, *55*, 2474-2477; c) D. Kurzbach, W. Hassouneh, J. R. McDaniel, E. A. Jaumann, A. Chilkoti, D. Hinderberger, *J Am Chem Soc* **2013**, *135*, 11299-11308; d) S. E. Reichheld, L. D. Muiznieks, F. W. Keeley, S. Sharpe, *Proc Natl Acad Sci* **2017,** 114, E4408-E4415.

[4] a) A. Leavesley, D. Shimon, T. A. Siaw, A. Feintuch, D. Goldfarb, S. Vega, I. Kaminker, S. Han, *Phys Chem Chem Phys* **2017**, *19*, 3596-3605; b) M. Kaushik, T. Bahrenberg, T. V. Can, M. A. Caporini, R. Silvers, J. Heiliger, A. A. Smith, H. Schwalbe, R. G. Griffin, B. Corzilius, *Phys Chem Chem Phys* **2016**, *18*, 27205-27218; c) G. Mathies, S. Jain, M. Reese, R. G. Griffin, *J Phys Chem Lett* **2016**, *7*, 111-116.

[5] a) E. Miclet, D. Abergel, A. Bornet, J. Milani, S. Jannin, G. Bodenhausen, *J Phys Chem Lett* **2014**, *5*, 3290-3295; b) R. Buratto, A. Bornet, J. Milani, D. Mammoli, B. Vuichoud, N. Salvi, M. Singh, A. Laguerre, S. Passemard, S. Gerber-Lemaire, S. Jannin, G. Bodenhausen, *ChemMedChem* **2014**, *9*, 2509-2515.

[6] a) N. Salvi, R. Buratto, A. Bornet, S. Ulzega, I. R. Rebollo, A. Angelini, C. Heinis, G. Bodenhausen, *J Am Chem Soc* **2012**, *134*, 11076-11079; b) Q. Chappuis, J. Milani, B. Vuichoud, A. Bornet, A. D. Gossert, G. Bodenhausen, S. Jannin, *J Phys Chem Lett* **2015**, *6*, 1674-1678.

[7] S. Ito, F. Hyodo, *Sci Rep* **2016**, *6*, 21407.

[8] D. M. Wilson, J. Kurhanewicz, *J Nucl Med* **2014**, *55*, 1567-1572.

[9]T. Wenckebach, *Essentials of Dynamic Nuclear Polarization*, Spindrift Publications, **2016**.

[10] D. Kurzbach, M. J. N. Junk, D. Hinderberger, *Macromol Rapid Comm* **2013**, *34*, 119-134.

[11] M. J. Junk, U. Jonas, D. Hinderberger, *Small* **2008**, *4*, 1485-1493.

[12] S. H. Petrosko, R. Johnson, H. White, C. A. Mirkin, *J Am Chem Soc* **2016**, *138*, 7443-7445.

[13] In a heterogeneous sample, an increase of the local concentration of paramagnetic species increases the number of nuclei that experience paramagnetic shifts. This phenomenon directly impacts the signal intensity and apparent polarizaion by decreasing the number of observable nuclei. In order to exclude contributions of this effect, each polarization has been calculated with respect to the NMR signal in thermal equilibrium. The local concentration of radicals and fraction of invisible nuclei can be considered to be similar for the hyperpolarised and reference spectra. Moreover, polarization profiles of samples which are less concentrated in paramagnetic species, and less subject to bleaching effects, also display a strong dependence on the ripening time (see Supporting Information).

[14] X. Ji, A. Bornet, B. Vuichoud, J. Milani, D. Gajan, A. J. Rossini, L. Emsley, G. Bodenhausen, S. Jannin, *Nat Commun* **2017**, *8*, 13975.

[15] D. Kurzbach, D. R. Kattnig, N. Pfaffenberger, W. Schartl, D. Hinderberger, *ChemistryOpen* **2012**, *1*, 211-214.

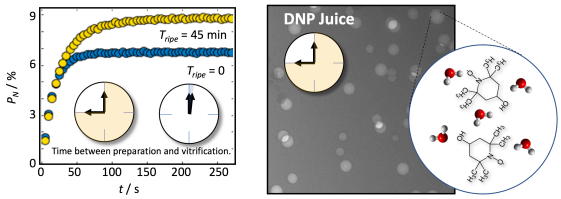

Spontaneous nanophase separation in water/glycerol mixtures can substantially impact the efficiency of dynamic nuclear polarization through the formation of water-rich vesicles with increased radical concentration.

*Emmanuelle M. M. Weber,[a] Giuseppe Sicoli,[b] Hervé Vezin,[b] Ghislaine Frébourg,[c] Daniel Abergel,[a] Geoffrey Bodenhausen,[a] Dennis Kurzbach[a]**

Sample Ripening through Nanophase Separation Impacts the Performance of Dynamic Nuclear Polarization